

Positioning Buried Utilities in Difficult Environments

Penghe Zhang¹, Craig Hancock¹, Lawrence Lau¹, Gethin Roberts², Huib de Ligt¹, Yiming Quan¹

¹ The University of Nottingham Ningbo China, 199 Taikang East Road, Ningbo, 315100, China

² Nottingham Geospatial Institute, The University of Nottingham, Triumph Road, Nottingham, NG7 2TU, UK

Abstract

Recently an increasing number of underground pipes have been established, particularly in city centres, for different applications such as sewage, electricity, gas, water and drainage. How to detect and make a precise 3-dimensional survey of underground pipelines has become a focused issue. This paper first of all reviews four trenchless detection technologies for locating buried utilities. Moreover, these trenchless detection technologies need to be integrated with positioning technologies to create maps for buried utilities. One of the most attractive positioning technologies for providing absolute global position is Global Navigation Satellite Systems (GNSS). However, a large percentage of buried utilities are in urban areas, which is an environment not ideal for GNSS positioning. This paper evaluates the availability and positioning accuracy of single and multi-GNSS constellations by carrying out experiments in a controlled environment. The results show that using combined GNSS systems improves availability in urban canyons compared with using GPS alone. Nevertheless, positioning accuracy may reduce with the combination of more satellites. Besides, the results show that using the Chinese BeiDou (BDS) system has a significant effect on the availability of positions in difficult environments. In addition, this paper describes an inertial based pipeline positioning technology called 'Ductrunner', which can locate and position the buried objects in spite of the material and depth with accurate coordinates of entry and exit points provided by GNSS. An approximately 30m long test pipeline has been installed to evaluate the performance of Ductrunner. The maximum positioning errors are found to be 8cm in horizontal plane and 4cm in height. This shows that this technology is promising for measuring deep pipes over relatively short distances.

Keyword: Buried utilities positioning; Multi-GNSS constellations; Positioning accuracy; Inertial based pipeline positioning technology; Difficult environments

1. Introduction

Recently an increasing number of underground pipes have been established, particularly in city centres. In the UK there are over 4 million km of buried pipes and cables, a combination of water, sewage, gas, electricity and drainage (Costello et al., 2007). A large number of underground pipelines increase the confusion of pipeline positioning. In order to prevent the damage of pipelines from excavation and construction work, accurate 3D pipeline mapping is important. However, the records of buried assets that utility companies relied on are potentially incomplete and inaccurate. How to detect and make a precise 3D dimensional survey of underground utilities has become a focused issue. In the UK, the Mapping the Underworld (MTU) project, which was a four year research program funded by Engineering and Physical Sciences Research Council (EPSRC), aimed to develop new solutions to find, locate and position buried utilities (Metje et al., 2007). In this project, four trenchless detection technologies are mainly used to detect underground utilities: vibro-acoustics, passive magnetic fields, low-frequency electromagnetic fields and ground penetrating radar.

After locating the buried utilities, it is necessary to create maps for recording the position of utilities by integrating with other positioning systems. One of the most attractive positioning technologies for providing absolute global position is Global Navigation Satellite Systems (GNSS) including USA's GPS, Russia's GLONASS, China's BeiDou (BDS), Europe's Galileo and Japan's QZSS (Roberts et al., 2007). The practical method to record the position of buried utilities is that after marking the markers on the ground where buried utilities are located by trenchless detection technologies, GNSS and Total station are usually utilised to record the positions of buried utilities. However, GNSS positioning relies heavily on the number of visible satellite and their geometry. A large number of buried utilities are in built up urban areas where sufficient number of visible satellites is not always possible and satellite geometry is not good due to the presence of trees and buildings. In addition, inertial navigation technology can be applied for pipeline positioning as well. Inertial based technology is a self-contained navigation technique. It is used to track the position and orientation of an object relative to a known starting point based on measurements acquired by accelerometers, gyroscopes and applying the dead reckoning (DR) principle (Savage, 1998). Nevertheless, the major drawback of INS is that navigation errors increase with time. INS errors are time dependent, which means the performance will degrade with time due to the error accumulation of inertial sensors.

This paper evaluates and compares ambiguity fixed solution availability, positioning precision and accuracy of single and multi-GNSS constellations by carrying out kinematic and static experiments in a controlled urban area environment at the University of Nottingham, Ningbo, China (UNNC). In addition, this paper assesses the performance of an inertial based pipeline positioning technology in a test pipeline.

2. Trenchless technologies for underground utilities detection

As described by Hao et al. (2012), the underground utilities network that serves our cities are the most complex in the world, and yet they are invisible from the ground surface. Due to the inability to

determine the position of buried utilities, open-cut methods are predominantly used to locate, replace or install utilities. However, it has been estimated that about 4 million holes are dug every year by utility companies to install and maintain subsurface assets, and the costs of direct trenching works are about £1.5 billion per year in the UK (McMahon et al., 2006). Furthermore, McMahon et al. (2006) points out that indirect costs including disruption to businesses and environmental damage are about £5.5 billion per year in the UK. Trenching to assess underground facilities destroys the carriageway and increases the cost. Trenchless technologies, unlike open-cut trenching for finding and locating buried utilities without digging a hole could save costs and can be more environmentally friendly (Royal et al., 2011). There are some advanced trenchless detection sensors widely used for locating buried assets without excavation such as, vibro-acoustics, passive magnetic fields, low-frequency electromagnetic fields and ground penetrating radar (Royal et al., 2011; Hao et al., 2012; Lester and Bernold, 2007).

3. GNSS overview

After determining the location of buried utilities by using the trenchless detection technologies, it is necessary to acquire and record the position of located utilities. Global Navigation Satellite Systems (GNSS) is one of the most attractive positioning technologies to provide absolute global position. Strictly speaking, there are only four GNSS constellations: US GPS, Russian GLONASS, Chinese BeiDou (BDS) and European Galileo. GPS and GLONASS are fully operational. GPS block IIF satellites are modernised to transmit a new signal L5 to improve precision and robustness of the system. Besides, the USA is currently building and launching block III GPS satellites to enhance quality of positioning. In contrast to GPS, GLONASS mainly uses Frequency Division Multiple Access (FDMA) techniques to distinguish GLONASS-M satellites. To increase compatibility and interoperability with other GNSS systems, GLONASS starts to use Code Division Multiple Access (CDMA) techniques on the new generation GLONASS-K satellites. BDS-2 has launched six Geostationary Earth Orbit (GEO) satellites, six Inclined Geosynchronous Satellite Orbit (IGSO) satellites and four Medium Earth Orbit (MEO) satellites. BDS has already contributed for positioning over China and neighbouring countries. Moreover, China started to develop the 3rd generation BeiDou system (BDS-3) which will offer a fully global navigation service by 2020. So far, 5 BDS-3 In Orbit Validation (IOV) satellites have been launched. There are currently twelve Galileo satellite: four IOV satellites and eight Full Operational Capability (FOC) satellites. In addition, there are Space Based Augmentation System (SBAS) and Regional Navigation Satellite Systems (RNSS) to improve the regional positioning performance. Quasi Zenith Satellite System (QZSS) is a Japanese satellite positioning system especially for usage in the Asia-Oceania regions, consisting of four geosynchronous satellites mainly in quasi-zenith orbits. Takahashi (2004) declares that the design concept is to have always at least one satellite near zenith over Japan to improve the positioning performance in urban canyons. Currently, Japan only launched one QZSS satellite "MICHIBIKI".

However, A large number of buried utilities are in built up urban areas where the performance of GNSS is constrained by an insufficient number of visible satellites, poor satellite geometry and multipath. The combination of GNSS systems increases the possible visible satellite number. There would be about 120 satellites in total if Galileo and BDS are fully operational in 2020 (Hancock et al.,

2009; [Gao and Enge, 2012](#)). Moreover, the geometry of satellites will be improved by integrating different GNSS constellations. [Rizos et al. \(2005\)](#) indicates that compared to GPS only, the visibility improvements of satellites for GPS/GLONASS, GPS/Galileo, and GPS/GLONASS/Galileo are respectively about 200%, 250%, and 350%. Meanwhile, the Positional Dilution of Position (PDOP) values of combined GNSS systems, which are determined by the geometry of satellites, are approximately half of the value of GPS only. In general, integration of GNSS systems increases the number of satellites, decreases the PDOP values and improves the positioning accuracy ([Hofmann-Wellenhof et al., 2008](#)). Extensive research has been conducted to investigate integration of Multi-GNSS constellations improves the availability, reliability and positioning accuracy. ([Truong and Tung, 2013](#); [Odijk and Teunissen, 2013](#); [Liu et al., 2016](#); [Li et al., 2010](#); [O’Keefe et al., 2009](#)). However, [Lau et al. \(2015\)](#) mentions that positioning accuracy may reduce when integrating more GNSS constellations in difficult environments due to a higher chance to get more multipath errors.

4. Inertial Navigation technology

Inertial Navigation Systems (INS) are self-contained navigation techniques. They are used to track the position and orientation of an object relative to a known starting point based on measurements acquired by accelerometers, gyroscopes and applying the dead reckoning (DR) principle ([Savage 1998](#)). An Inertial Measurement Unit (IMU) typically contains three orthogonal accelerometers measuring linear accelerations and three orthogonal gyroscopes measuring angular rates. Dead reckoning principle determines the position of the object from previous position and the measured accelerations and angular rotations. The integration of acceleration obtains velocity and a second integration provides position. Angular rates are integrated to get the attitude of the object in terms of pitch, roll and yaw.

There are two types of Inertial Navigation Systems: stable platform systems and strapdown systems. The difference between the two types is the frame of reference where accelerometers and gyroscopes operate. The inertial units of stable platform systems align with the global frame. Unlike the stable platform systems, the inertial sensors in strapdown systems are rigidly mounted to the device. Compared with the stable platform systems, strapdown systems decrease the mechanical complexity and tend to be physically smaller than the stable platform systems ([Titterton and Weston, 1997](#)). Strapdown systems lead the trend of inertial navigation systems. However the output measurements of strapdown systems are in the body frame rather than global frame. The integration of rate gyroscopes gives orientation. Using known orientation, accelerations are processed into global coordinates to track position. The algorithm of a strapdown inertial navigation system is shown in Figure 1.

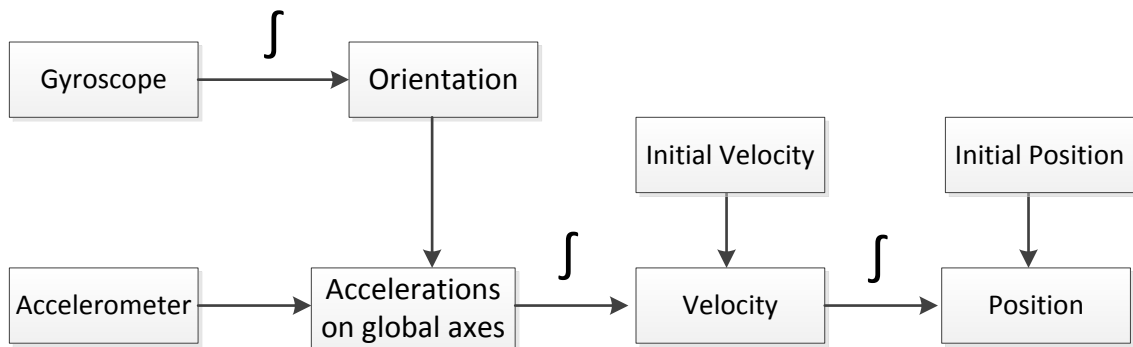


Figure 1 A strapdown Inertial Navigation Algorithm.

There are many types of gyroscopes and accelerometers such as mechanical gyroscopes, optical gyroscopes, mechanical accelerometers and solid state accelerometers. Compared with these sensors, micro-machined electromechanical systems (MEMS) sensors have the advantages of small size, low weight, low power consumption, short start up time and cheap to manufacture. However MEMS sensors are less accurate than optical devices. MEMS gyroscopes and accelerometers have errors including random noise, biases, scale factor, cross coupling and temperature sensitivity.

Unlike GNSS systems, INS, that primarily measure position, velocity and attitude, are autonomous systems and do not depend on external electromagnetic signals or visibility conditions. Moreover, INS can operate in any difficult environments, for instance, urban canyons, and achieve high accuracy in the short term (Taha et al., 2008). Nevertheless, the major drawback of INS is that navigation errors increase with time. Besides the acquisition costs, operations costs and maintenance costs of INS are higher than GNSS receivers (Grewal et al., 2013). INS errors are time dependent, so performance will degrade with time because of the error accumulation of inertial sensors. Groves (2008) explains that the errors of accelerometers and gyroscopes increase linearly over time. However, to estimate position, after double integration of accelerations, the error increases rapidly over long periods of time. To overcome the IMU drift, other sensors, such as odometer, speedometer and GNSS, can be combined with IMU to gather additional information for speed, distance, heading and position (Zhang et al., 2016).

5. Multi-GNSS test design and data collection

Multi-GNSS kinematic and static experiments were carried out on the campus at UNNC, where it is possible to track multi-GNSS signals including GPS, GLONASS, Galileo, BDS and QZSS. In the kinematic test, the reference station used a Leica GS10 receiver and JAVAD Sigma receiver, which were connected to a Leica AR20 choke-ring antenna on the roof of the Science and Engineering Building (SEB) through a signal splitter. The roving receivers used were a Leica GS10 receiver that is capable of receiving GPS and GLONASS signals and a JAVAD Sigma receiver that can track GPS, GLONASS, QZSS and Galileo signals connected to one Leica AS10 lightweight antenna through a signal splitter. These instruments were fixed on a trolley (Figure 2). The trolley was slowly pushed around the dormitory area of UNNC (Figure 3), a few hundred meters away from the reference station. This

area comprises many buildings with relatively narrow streets between them and can be considered similar to a city centre environment. Data was collected from UTC 04:32:10 to 05:37:10 on October 28th 2013. Results and analysis of this experiment are presented in Section 6.



Figure 2 Rovers fixed on a trolley.

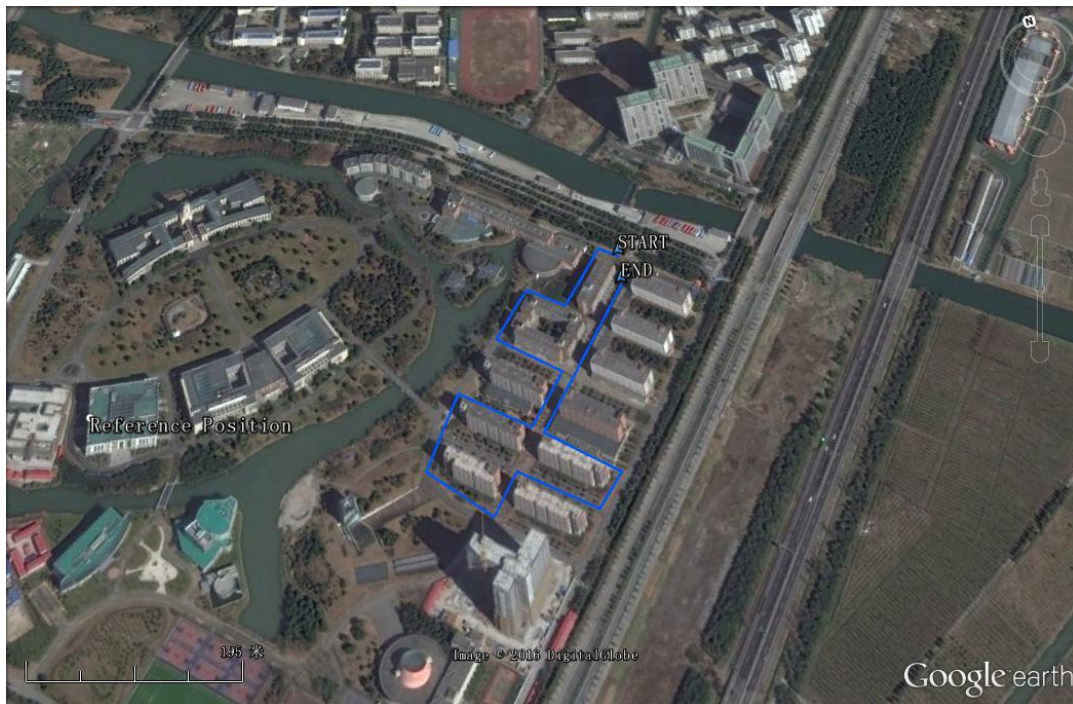


Figure 3 Trajectory of the kinematic test.

In the static test, 28 markers were installed on the campus in a variety of scenarios, from open sky environments to deep dense urban canyon environments (Figure 4). To obtain accurate coordinates for all the markers, firstly, these markers were surveyed by using a total station and a digital level to obtain the local coordinates. Secondly, four markers: 21, 23, 4 and 29, in open sky environments, were chosen to do static GPS surveying for 10 hours at the same time by using 4 Leica GS10 receivers. Thirdly, after acquiring the GPS coordinates of these 4 markers, the GPS coordinates were transferred to a local coordinate system aligned with the geographic directions at point 21, which is set as origin. Finally the local coordinates of 21 and 23 are inputted to the total station traverse network to calculate the coordinates of others markers including 4 and 29 by using the Starnet software. It has been found that the maximum horizontal error of points 4 and 29 calculated in traverse network is 0.007m (Table 1). As points 4 and 29 are in the boundary of the network, the maximum horizontal errors for other markers should be less than 0.007m.



Figure 4 The test network at the University of Nottingham, Ningbo, China.

Table 1 Horizontal error in the traverse network.

Points	E(m)	N(m)
4	0.007	0.006
29	0.004	0.007

In the static test, a JAVAD Triumph VS receiver, capable of receiving GPS, GLONASS, BDS, QZSS and Galileo satellite signals, was placed on each marker for 3 minutes and data was collected at 1Hz. The

reference station was a JAVAD Triumph VS receiver connected to a Leica AR20 choke-ring antenna on the roof of SEB. This experiment commenced on 2014/8/27 09:20:30. For each marker, the number of visible satellites, Positional Dilution of Precision (PDOP) value, ambiguity fixed solution availability and positioning accuracy are analysed and presented in Section 6. The GNSS positioning results of markers are compared with the positions calculated from the test network. 28 markers are divided into 5 categories according to the environment around each particular (Table 2).

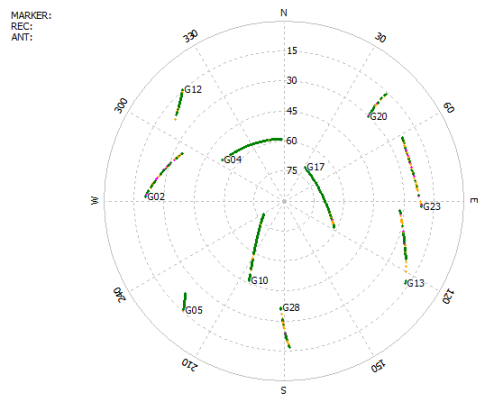
Table 2 Definition of area categories with associated numbers in the test network.

Category Number	Scenario Definition	Marker Numbers
1	Open sky	4, 9, 21, 23
2	At least 180 degrees no buildings	22, 31, 32, 45, 46, 48, 49
3	90 degrees no buildings; wide street	1, 33, 34, 35, 38, 41, 42, 47
4	90 degrees no buildings; narrow street	2, 3, 36, 37, 44
5	Multiple buildings or obstructions	39, 40, 43, 50

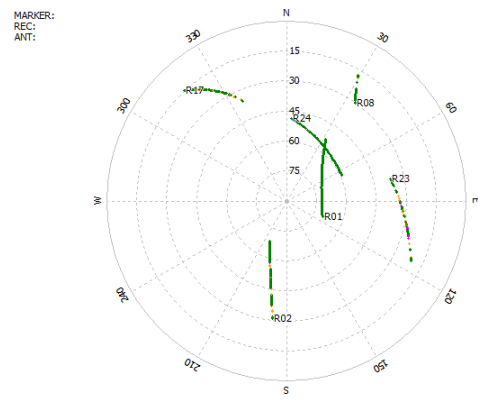
6. Multi-GNSS positioning results in urban environments.

For the GNSS analysis, the elevation mask angle is 15 degrees. RTKLIB (version 2.4.2) software is used to process the GNSS positioning results. RTKLIB is an open source program package for GNSS data process including GPS, GLONASS, BDS, Galileo, QZSS and SBAS (Takasu, 2014). Root Mean Square (RMS) error is used to analyse the positioning accuracy of different GNSS constellations and combinations.

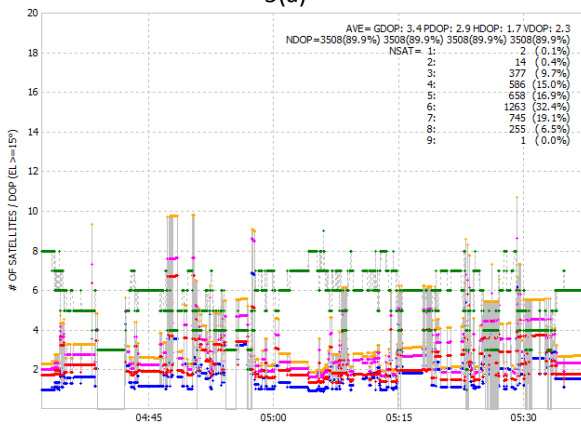
6.1 Results of Leica GS10 receiver in the kinematic test



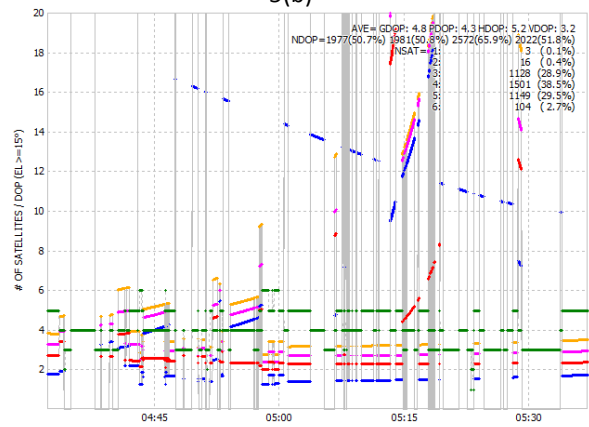
5(a)



5(b)



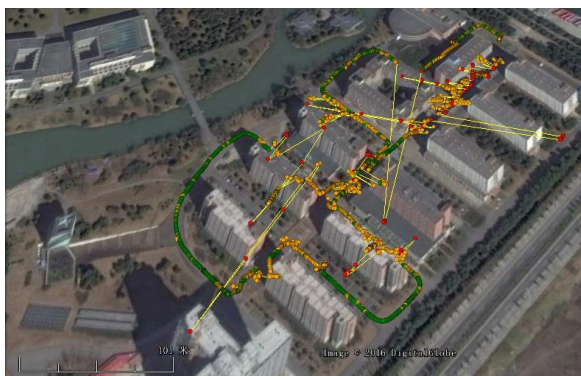
5(c)



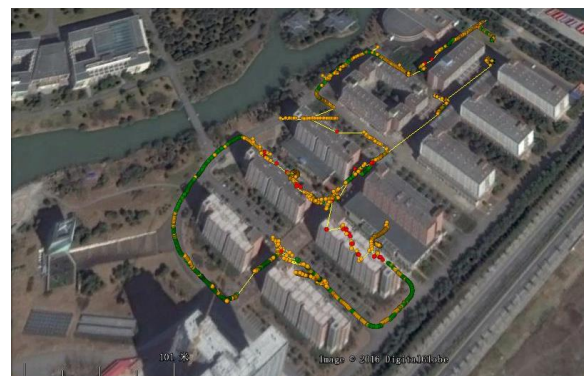
5(d)

Figure 5 The number of visible satellites, DOP values and sky plots of GPS and GLONASS.

Figure 5(a) and 5(b) show the sky plots of GPS and GLONASS satellites respectively (G: GPS, R: GLONASS). Figure 5(c) and 5(d) show the number of visible satellites and DOP values of GPS and GLONASS respectively (Green: The number of visible GPS satellite; Blue: HDOP; Red: VDOP; Pink: PDOP; Yellow: GDOP). Figure 5 shows that during the test period, the number of visible GPS satellites is equal or more than 4 for approximately 90% of the test period, the number of visible GLONASS satellites equal to or more than 4 for about 70% of the test period. In addition, the average PDOP values of GPS and GLONASS are respectively 2.9 and 4.3, which means the satellite geometry of GPS is better than GLONASS.



6(a) GPS



6(b) GLONASS

Figure 6 Comparison of GPS and GLONASS positioning results.

Figure 6(a) and 6(b) show GPS and GLONASS positioning result respectively. (Green: ambiguity fixed solution; Yellow: ambiguity float solution; Red: stand-alone solution). Figure 6 compares the positioning results of GPS and GLONASS. It shows that most of the ambiguity fixed solutions are on the path outside of buildings. On the path between buildings, GPS can only provide ambiguity float solutions, sometimes even stand-alone solutions. Compared with GPS, GLONASS provides fewer ambiguity float solutions on the path between buildings.

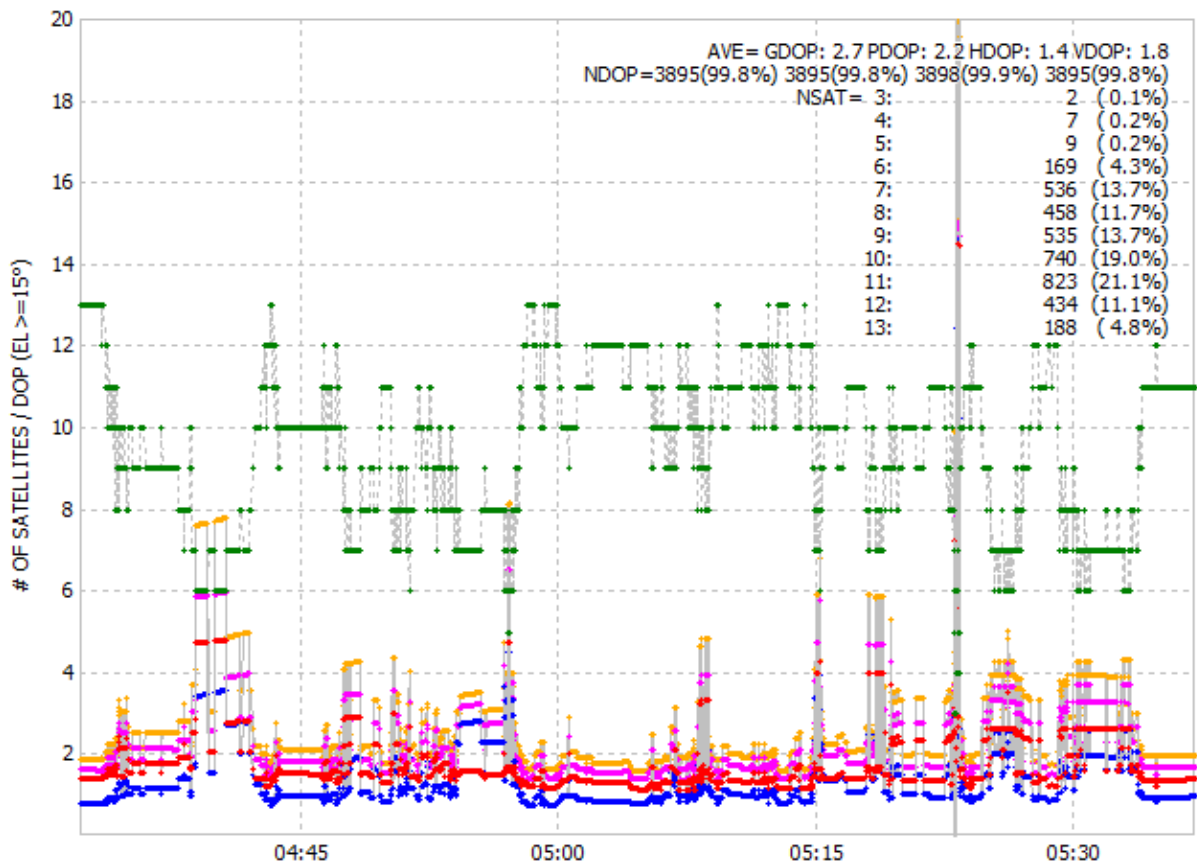


Figure 7 The number of visible GPS+GLONASS satellites and DOP values.

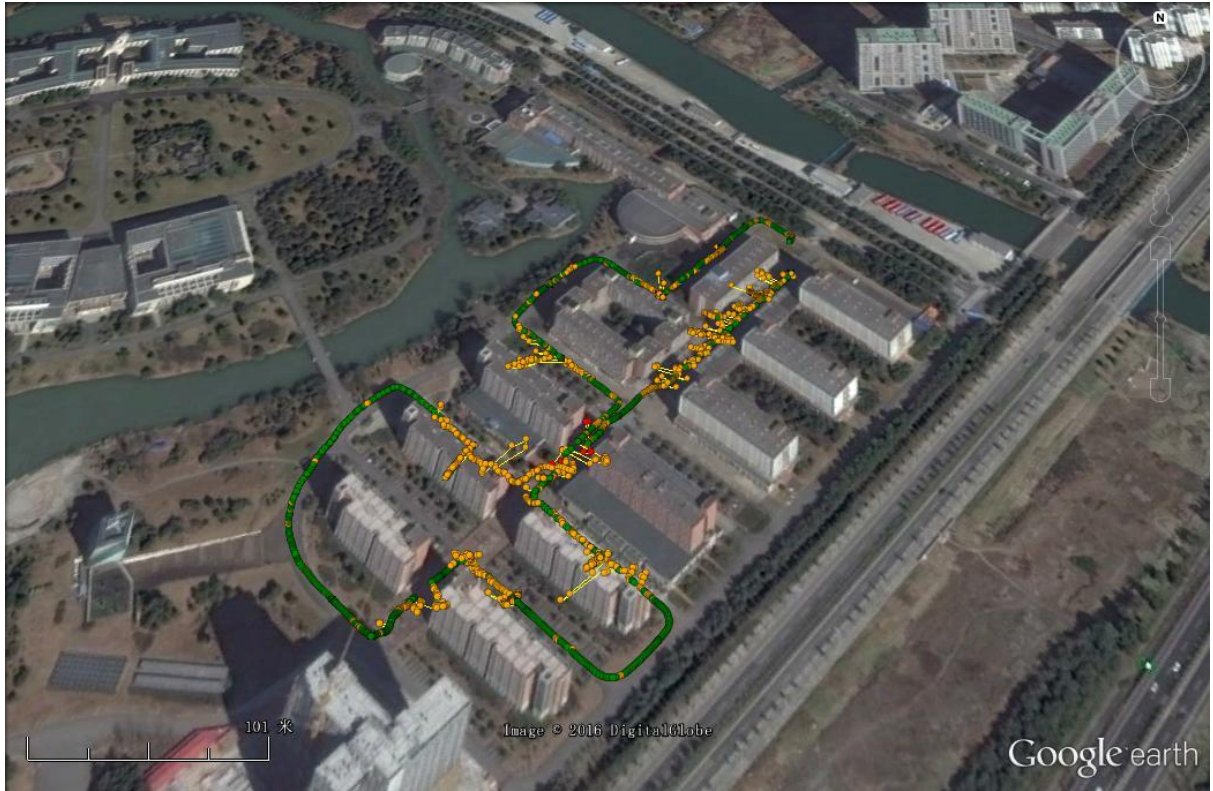


Figure 8 GPS+GLONASS positioning results.

Comparing Figure 7 with Figure 5, the combination of GPS and GLONASS increases the number of visible satellites to more than 5 in 99.5% of the test period. Moreover, the average PDOP reduces to 2.2. By comparing Figure 8 with Figure 6, it shows that the GPS+GLONASS positioning results are much better than GPS or GLONASS alone with more ambiguity fixed solutions. However, there are still only ambiguity float solutions in narrow streets.

Table 3 Positioning results of the Leica GS10 receiver.

Receiver	GNSS constellation	Solution Quality				Standard deviations (m)		
		Fixed	Float	Single	No solution	sdn	sde	sdu
GS10	GPS	963(24.7%)	2437(62.5%)	82(2.1%)	418(10.7%)	0.794	1.027	1.423
	GLONASS	720(18.5%)	1262(32.4%)	40(1.0%)	1878(48.2%)	1.414	1.531	2.300
	GPS/GLONASS	1785(45.8%)	2095(53.7%)	10(0.3%)	10(0.3%)	0.523	0.488	0.847

Table 3 shows that GPS can provide about 90% positioning solutions in the test period, much more than GLONASS, which can only provide only 52% positioning solutions. However, for GPS, only 24.7% solutions are ambiguity fixed solutions, for GLONASS, only 18.5% solutions are ambiguity fixed. In addition, the most ambiguity fixed solutions are in open sky environments. There are only a few ambiguity fixed solutions in dense urban area. By integrating GPS and GLONASS, the number of visible satellites is more than 4 in the whole test period. The combined system can provide the

whole positioning solutions in the test period. And it much improves the ambiguity fixed solutions to 45.8%. The positioning result is better than GPS or GLONASS alone.

6.2 Results of JAVAD Sigma receiver in the kinematic test Category

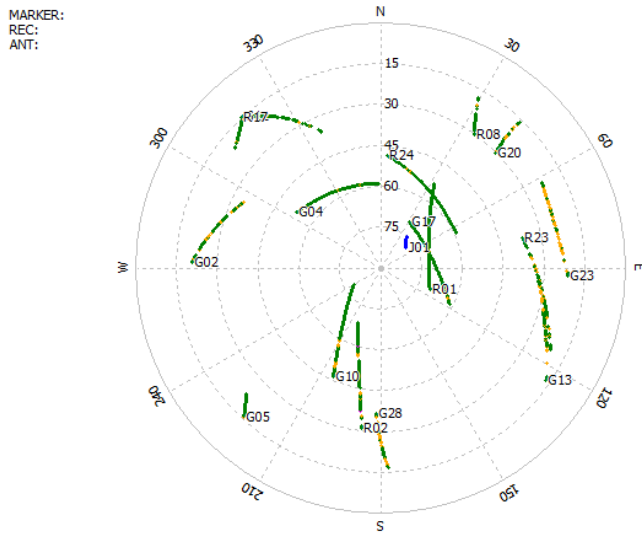
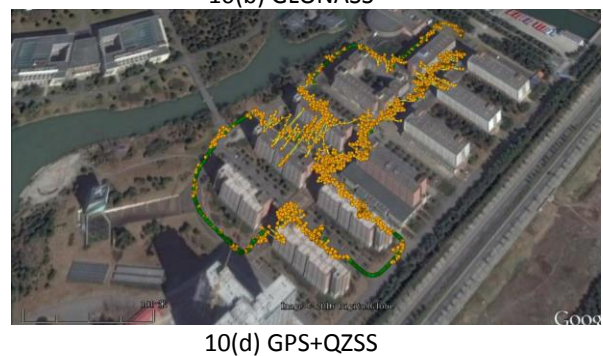
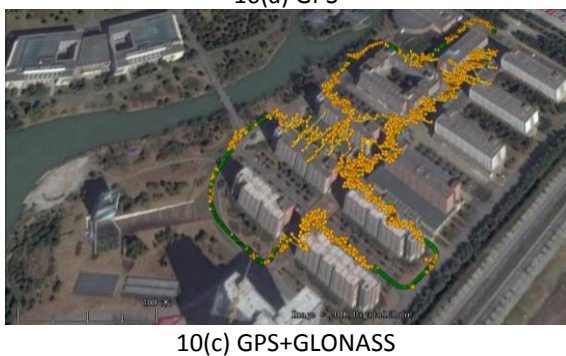
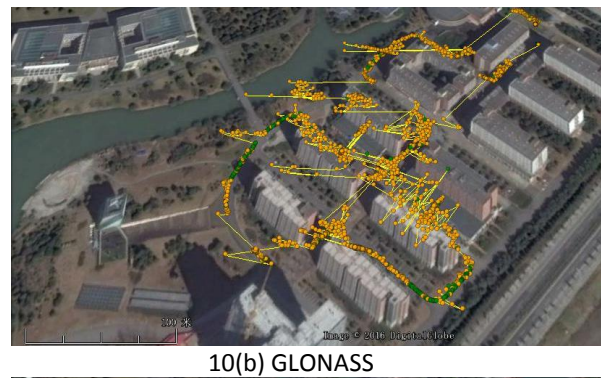
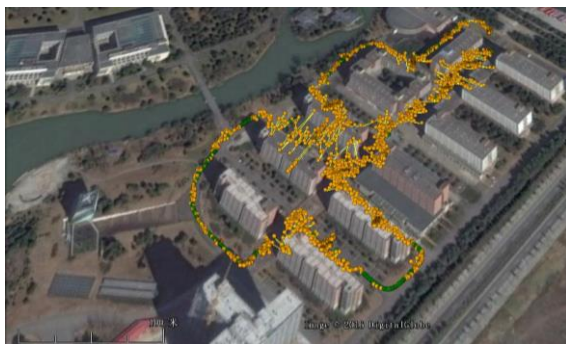


Figure 9 Sky plot of visible GNSS satellites (G: GPS, R: GLONASS and J: QZSS).





10(e) GLONASS+QZSS



10(f) GPS+GLONASS+QZSS

Figure 10 Positioning results of different GNSS constellations.

Table 4 Positioning results of the JAVAD Sigma receiver.

Receiver	GNSS	Solution Quality				Standard deviation(M)		
		Fixed	Float	Single	No solution	sdn	sde	sdu
SIGMA	GPS	473(12.1%)	3311(84.9%)	0(0.0%)	116(3.0%)	0.595	0.530	1.126
	GLONASS	507(13.0%)	2093(53.7%)	0(0.0%)	1300(33.3%)	1.340	1.598	2.240
	GPS/GLONASS	986(25.3%)	2881(73.9%)	0(0.0%)	33(0.8%)	0.442	0.434	0.864
	GPS/QZSS	914(23.4%)	2894(74.2%)	0(0.0%)	92(2.4%)	0.512	0.457	0.902
	GLONASS/QZSS	573(14.7%)	2472(63.4%)		855(21.9%)	1.084	1.720	2.136
	GPS/GLONASS/QZSS	1166(29.9%)	2705(69.4%)	0(0.0%)	29(0.7%)	0.397	0.390	0.753

Figure 10 and Table 4 show that for the JAVAD Sigma receiver, GPS and GLONASS provide similar percentage of ambiguity fixed solutions about 13%. But GPS provides more ambiguity float solutions than GLONASS. Combining GPS and GLONASS, the number of ambiguity fixed solutions doubled. In addition, integrating GPS with only one QZSS satellite, which elevation angle is above 75 degrees (shown in Figure 10) during the test provides similar results compared with GPS and GLONASS combination. Integrating GPS, GLONASS and QZSS obtains 29.9% ambiguity fixed solutions throughout the test period. The positioning results of the Leica GS10 and JAVAD Sigma receivers show that GPS positioning result is better than GLONASS. Integrating GPS and GLONASS improves the percentage of ambiguity fixed solutions to about twice than GPS alone. However, almost all of the ambiguity fixed solutions are in open sky environment; even with a vastly improved availability of satellites it is still difficult to obtain ambiguity fixed solutions in urban areas.

6.3 Static test results and analysis

In the static test, the number of visible satellites, PDOP values, ambiguity fixed solution availability and positioning accuracy of different GNSS constellations including GPS, GLONASS, BDS, GPS+GLONASS, GPS+BDS and GPS+GLONASS+BDS are analysed for the markers in different Categories.

6.3.1 Positioning results for the markers in Category 1

The 1st test on marker 21 was from 2014/8/27 09:20:30 to 09:23:32. Figure 11(a) shows all the five BDS satellites are in the South direction of marker 21 and the PDOP value is 12.8 (shown in Figure

12(a)), which leads to the RMS positioning error in North direction of 0.029m (shown in Figure 13(a)). To verify it is caused by the geometry of BDS Satellite, another test on marker 21 was from 2014/08/28 02:45:39 to 2014/08/28 02:48:45. In the 2nd test, Figure 11(b) shows that there are two BDS satellites (C08 and C11) in the North direction and five BDS satellites (C01, C03, C04, C07, C10) in the South direction of marker 21. Moreover Figure 12(b) shows the BDS satellite PDOP value is 9.7. Moreover the RMS positioning error in North direction is 0.008m (shown is Figure 13(b)).

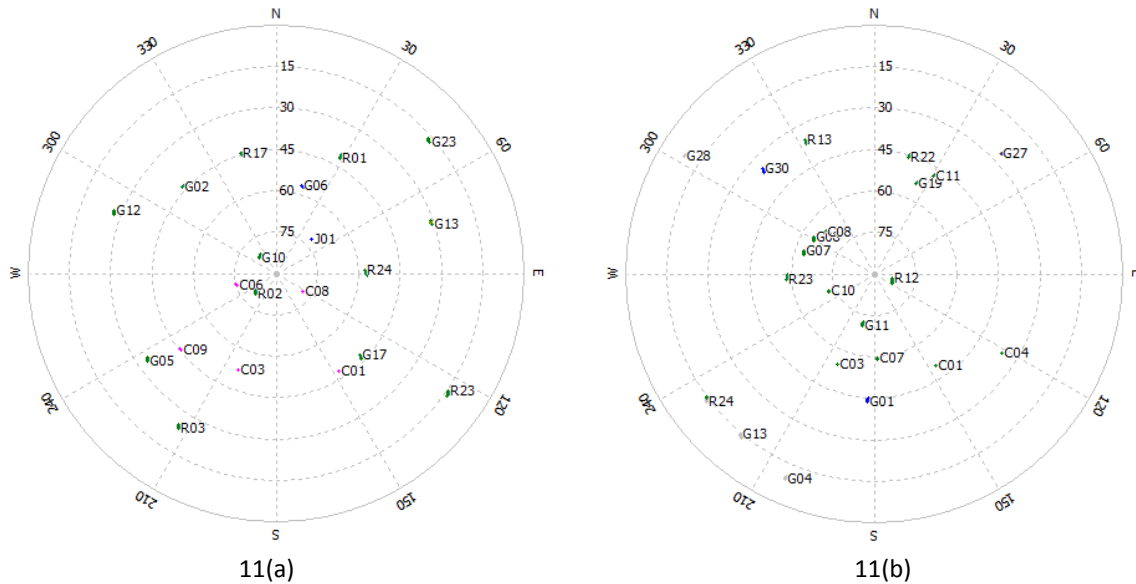


Figure 11 Sky plots of visible GNSS satellites on marker 21 in the two tests (C: BDS).

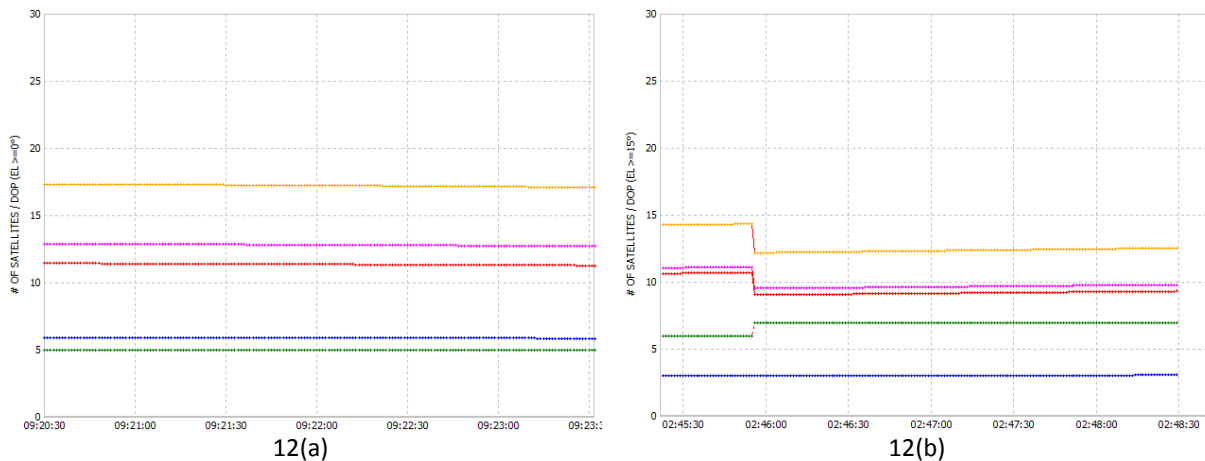
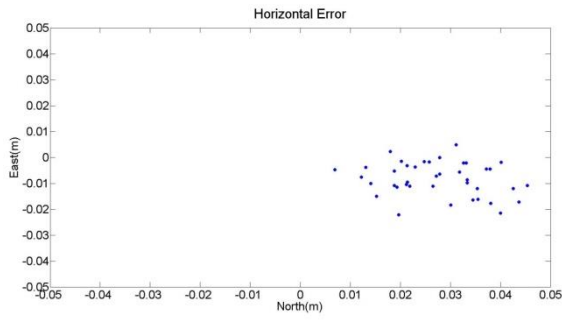
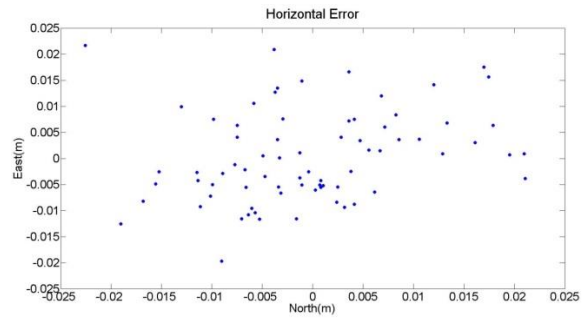


Figure 12 The number of visible BDS satellites and DOP values on marker 21 in the two tests (Pink: PDOP).



13(a)



13(b)

Figure 13 The horizontal positioning error of BDS on marker 21 in the two tests.

Table 5 The number of visible satellites and PDOP values of different constellations on markers in Category 1 (G/G: GPS+GLONASS; G/B: GPS+BDS; G/G/B: GPS+GLONASS+BDS).

Marker	GPS		GLONASS		BDS		G/G		G/B		G/G/B	
	No	PDOP	No	PDOP	No	PDOP	No	PDOP	No	PDOP	No	PDOP
21(1st)	8	2.1	7	3.2	5	12.8	15	1.6	13	1.7	20	1.4
21(2nd)	7	3	5	3.3	7	9.7	12	1.7	14	2.5	19	1.6
4	8	2	5	3.6	7	6.7	13	1.7	15	1.5	20	1.4

Table 6 The percentage of ambiguity fixed solutions for different GNSS constellations on markers in Category1.

Marker	Fixed Solution					
	GPS	GLONASS	BDS	G/G	G/B	G/G/B
21(1st)	100.0%	50%	22.0%	100%	100.0%	75.6%
21(2nd)	100.0%	47%	41.0%	62.2%	100.0%	50.0%
4	100.0%	44%	87.0%	98.9%	78.0%	91.7%

Table 7 The horizontal and vertical positioning errors of different constellations on markers in Category 1.

Marker	GPS		GLONASS		BDS		G/G		G/B		G/G/B	
	H(m)	V(m)	H(m)	V(m)	H(m)	V(m)	H(m)	V(m)	H(m)	V(m)	H(m)	V(m)
21(1st)	0.005	0.046	0.006	0.073	0.029	0.109	0.005	0.049	0.006	0.052	0.005	0.048
21(2nd)	0.002	0.045	0.009	0.051	0.008	0.050	0.002	0.062	0.003	0.059	0.002	0.061
4	0.005	0.059	0.005	0.065	0.004	0.073	0.005	0.089	0.007	0.086	0.006	0.086

Table 5, 6 and 7 show that in open sky environments, GPS provides 100% ambiguity fixed solutions in the test period. The average horizontal and vertical positioning errors are 0.004m and 0.050m respectively. Due to the Frequency Division Multiple Access (FDMA) techniques used by GLONASS, it is difficult to get ambiguity fixed solutions even in open sky environments (Liu et al., 2016). In this test, the percentage of ambiguity fixed solutions for GLONASS is 47%. The horizontal and vertical positioning errors are 0.007m and 0.063m respectively. During the test, BDS has 5 GEO satellites, 5 IGSO satellites and 4MEO satellite, and can only provide positioning services in Asia Pacific region. Due to the relatively low number of MEO satellite and GEO satellite always in the same area of the sky, the geometry of satellites is poor, which leads to the PDOP values of BDS being larger, on average, than GPS and GLONASS. Sometimes the poor geometry of satellites much effects the positioning accuracy, for instance, in the first test on marker 21, all of the five satellites (2 GEO, 3IGSO) are in the south direction of marker 21, which leads to PDOP values of 12.8 and the RMS positioning error in north south direction is 0.029m . BDS provides 64% ambiguity fixed solutions for the two markers in open sky environments, which is probably due to the geometry of BDS satellites. The horizontal and vertical positioning errors are 0.006m and 0.062m respectively. The integration of GPS, GLONASS and BDS improves the satellite geometry compared with single GNSS constellation. Adding GLONASS and BDS to GPS, the positioning result is better than GLONASS and BDS alone. However, it increases the number of wrong ambiguity fixes, which results in the positioning error is slightly larger than GPS alone (Shown in Table 7).

6.3.2 Positioning results for the markers in Category 2

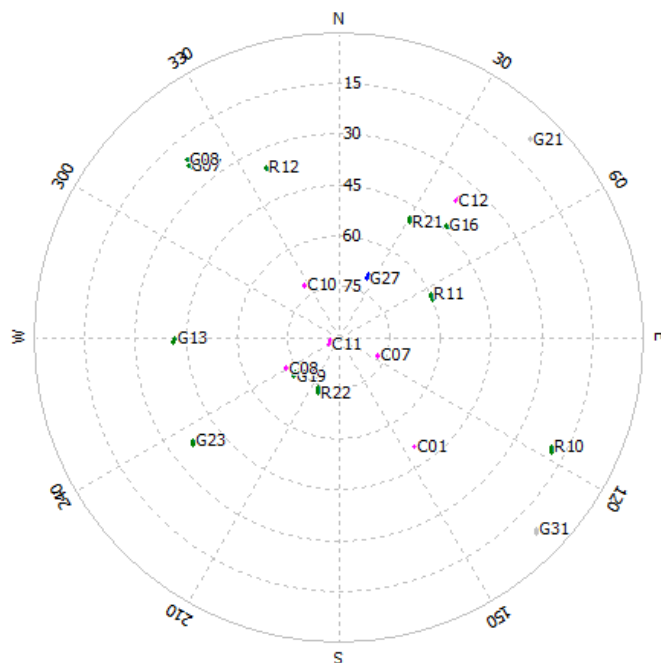


Figure 14 Sky plot of GNSS satellites on marker 49.

Table 8 The number of visible satellites and DOP values on the markers in Category 2.

Marker	GPS		GLONASS		BDS		G/G		G/B		G/G/B	
	No	PDOP	No	PDOP	No	PDOP	No	PDOP	No	PDOP	No	PDOP
22	7	2.5	5	2.8	6	9.3	12	1.8	13	2.1	18	1.6
31	6	3.9	6	2.3	7	10.2	12	1.7	13	2.8	19	1.5
32	7	2.4	5	3.1	5	12.3	12	1.6	12	1.7	17	1.6
45	8	2.7	5	2.9	6	7.0	13	1.8	14	1.7	19	1.4
46	8	2.6	5	2.8	7	6.8	13	1.7	15	1.7	20	1.4
48	7	2.2	5	3.0	6	7.1	12	1.9	13	1.8	18	1.6
49	7	3.8	5	2.9	7	4.4	12	1.6	14	2.0	19	1.4

Table 9 The percentage of ambiguity fixed solutions for different GNSS constellations on the markers in Category 2.

Marker	Fixed Solution					
	GPS	GLONASS	BDS	G/G	G/B	G/G/B
22	0.0%	0.0%	2.0%	1.1%	34.4%	0.0%
31	44.0%	0.0%	41.0%	67.8%	100.0%	1.0%
32	14.0%	0.0%	8.0%	27.0%	19.0%	26.0%
45	9.0%	17.0%	100.0%	0.0%	21.7%	0.0%
46	67.0%	0.0%	84.0%	17.8%	51.1%	0.0%
48	67.0%	0.0%	5.0%	68.3%	15.6%	15.0%
49	100.0%	2.0%	20.0%	60.0%	73.9%	39.0%

Table 10 The horizontal and vertical positioning errors of different constellations on markers in Category 2.

Marker	GPS		GLONASS		BDS		G/G		G/B		G/G/B	
	H(m)	V(m)	H(m)	V(m)	H(m)	V(m)	H(m)	V(m)	H(m)	V(m)	H(m)	V(m)
22	-	-	-	-	0.004	0.069	0.018	0.032	0.006	0.050	-	-
31	0.008	0.066	-	-	0.009	0.023	0.007	0.061	0.010	0.061	0.007	0.060
32	0.010	0.063	-	-	0.009	0.063	0.008	0.071	0.009	0.064	0.008	0.069
45	0.010	0.080	0.095	0.028	0.013	0.122	-	-	0.010	0.090	-	-
46	0.010	0.064	-	-	0.005	0.029	0.001	0.069	0.003	0.048	-	-
48	0.017	0.075	-	-	0.016	0.007	0.022	0.071	0.006	0.055	0.009	0.048
49	0.002	0.079	0.148	0.663	0.002	0.061	0.003	0.073	0.001	0.071	0.002	0.072

Table 8 shows that the average number of visible GPS, GLONASS and BDS satellites are respectively 7.1, 5.1 and 6.3 in Category 2. And the PDOP values are less than 4 for GPS and GLONASS. However, the average BDS PDOP value is larger than 8. Integration of GPS, GLONASS and

BDS much improves the satellite geometry and decreases the PDOP values to less than 2. Table 9 and 10 show that GLONASS has difficulty acquiring ambiguity fixed solutions. There are only two markers that are able to obtain ambiguity fixed solutions inside a few seconds. The positioning accuracy is at centimetre/decimetre level. GPS provides ambiguity fixed solutions for 86% of the markers (6 out of 7) in. However, GPS can only provide an average of 43% fixed solutions for each marker. The average horizontal and vertical positioning errors are 0.010m and 0.071m respectively. In the test period, due to the high elevation angles of BDS IGSO satellites, for instance, the elevation angles of four BDS IGSO satellites above marker 49 are higher than 70 degrees (Shown in Figure 14), BDS provides ambiguity fixed solutions for all the markers, and the percentage of fixed solutions is 37%. The average horizontal and vertical positioning errors are 0.008m and 0.053m respectively. The vertical positioning accuracy is much better than GPS. The GPS+GLONASS, GPS+BDS and GPS+BDS+GLONASS provide average 34.6%, 45.1% and 11.6% ambiguity fixed solutions and the RMS horizontal and vertical positioning errors are 0.010m and 0.063m, 0.006m and 0.063m, 0.007m and 0.062m respectively.

6.3.3 Positioning results for the markers in Category 3

Table 11 The number of visible satellites and DOP values for the markers in Category 3.

Marker	GPS		GLONASS		BDS		G/G		G/B		G/G/B	
	No	PDOP	No	PDOP	No	PDOP	No	PDOP	No	PDOP	No	PDOP
1	6	5.5	5	3	6	10.5	11	1.7	12	2.4	17	1.4
33	5	5.2	5	3.1	5	8	10	2.4	10	2.9	15	2.1
34	6	3.6	5	3	5	13.2	11	2.2	11	3	16	2
35	8	2.3	5	2.9	5	14.4	13	1.8	13	1.9	18	1.4
38	7	2.8	5	3.1	4	20	12	2.3	11	2.1	16	1.7
41	6	3	4	3.9	6	12.8	10	2.3	12	2.1	16	1.9
42	5	6.9	5	3.1	4	13.8	10	2.4	9	3.2	14	1.8
47	5	7	6	2.3	6	11.5	11	1.8	12	2.2	17	1.1

Table 12 The percentage of ambiguity fixed solutions for different GNSS constellations in Category 3.

Marker	Fixed Solution					
	GPS	GLONASS	BDS	G/G	G/B	G/G/B
1	0.0%	0.0%	1.0%	0.0%	11.7%	1.1%
33	92.0%	0.0%	0.0%	1.6%	100.0%	37.8%
34	1.0%	0.0%	46.0%	0.0%	5.6%	0.0%
35	0.0%	0.0%	0.0%	0.0%	18.9%	3.9%
38	52.0%	7.0%	0.0%	98.9%	91.1%	74.4%

41	0.0%	0.0%	12.0%	0.0%	0.0%	0.0%
42	0.0%	0.0%	0.0%	0.0%	0.0%	0.0%
47	4.0%	0.0%	0.0%	0.0%	48.9%	0.0%

Table 13 The horizontal and vertical positioning errors of different constellations on markers in Category 3.

Marker	GPS		GLONASS		BDS		G/G		G/B		G/G/B	
	H(m)	V(m)	H(m)	V(m)	H(m)	V(m)	H(m)	V(m)	H(m)	V(m)	H(m)	V(m)
1	-	-	-	-	0.011	0.017	-	-	0.008	0.051	0.003	0.042
33	0.008	0.079	-	-	0.019	0.084	0.008	0.086	0.008	0.084	0.007	0.077
34	0.024	0.070	-	-	0.011	0.078	-	-	0.025	0.049	-	-
35	-	-	-	-	-	-	-	-	0.007	0.080	0.009	0.07
38	0.010	0.058	0.019	0.060	-	-	0.010	0.058	0.005	0.061	0.005	0.064
41	-	-	-	-	0.014	0.014	-	-	-	-	-	-
42	-	-	-	-	-	-	-	-	-	-	-	-
47	0.013	0.050	-	-	-	-	-	-	0.008	0.070	-	-

The 8 Markers in Category 3 are in semi-dense urban environments, the number of visible GPS, GLONASS and BDS decreases to 6, 5, and 5.1. Due to buildings around the markers, the PDOP values increase to 4.5, 3.1 and 12.0 respectively (Shown in Table 11). Table 12 and 13 show that GPS provides ambiguity fixed solutions for 50% of the markers (4 out of 8), and the fixed solution percentage is 18.6% for each marker. The horizontal and vertical positioning errors are 0.009m and 0.074m. BDS provides ambiguity fixed solutions of 37.5% of the markers (3 out of 8), and the fixed solution percentage is 7.4% for each marker. The horizontal and vertical positioning errors are 0.014m and 0.048m. GLONASS only provides 7% ambiguity fixed solutions for one marker, and the horizontal and vertical positioning errors are 0.019m and 0.060m. The GPS+GLONASS, GPS+BDS and GPS+BDS+GLONASS provide an average of 12.6%, 34.5% and 14.7% ambiguity fixed solutions and the RMS horizontal and vertical positioning errors are 0.009m and 0.072m, 0.010m and 0.066m, 0.006m and 0.063m respectively.

6.3.4 Positioning results for the markers in Category 4

Table 14 The number of visible satellites and DOP values for the markers in Category 4.

Marker	GPS		GLONASS		BDS		G/G		G/B		G/G/B	
	No	PDOP	No	PDOP	No	PDOP	No	PDOP	No	PDOP	No	PDOP
2	5	4.3	5	3	6	11.2	10	1.2	11	2.7	16	1.7
3	5	3.9	4	3.2	4	50	9	2.2	8	2.7	13	1.8
36	6	2.7	5	2.9	4	29	11	2.3	9	3.2	15	1.6

37	6	2.6	4	6.5	5	13.9	10	2.4	9	2.7	15	1.9
44	7	2.8	4	3.3	6	10.8	11	2.3	10	1.9	17	1.7

Table 15 The percentage of ambiguity fixed solutions for different GNSS constellations in Category 4.

Marker	Fixed Solution					
	GPS	GLONASS	BDS	G/G	G/B	G/G/B
2	7.0%	0.0%	6.0%	0.0%	24.4%	0.0%
3	4.0%	0.0%	0.0%	25.0%	0.0%	2.8%
36	0.0%	0.0%	0.0%	0.0%	0.0%	0.0%
37	0.0%	0.0%	0.0%	0.0%	0.0%	0.0%
44	0.0%	0.0%	34.0%	0.0%	0.0%	0.0%

Table 16 The horizontal and vertical positioning errors of different constellations on markers in Category 4.

Marker	GPS		GLONASS		BDS		G/G		G/B		G/G/B	
	H(m)	V(m)	H(m)	V(m)	H(m)	V(m)	H(m)	V(m)	H(m)	V(m)	H(m)	V(m)
2	0.007	0.006	-	-	0.015	0.127	-	-	0.009	0.011	-	-
3	0.032	0.082	-	-	-	-	0.025	0.067	-	-	0.007	0.071
36	-	-	-	-	-	-	-	-	-	-	-	-
37	-	-	-	-	-	-	-	-	-	-	-	-
44	-	-	-	-	0.008	0.071	-	-	-	-	-	-

The 5 markers in Category 4 are in dense urban environments. The number of visible GPS, GLONASS and BDS are 5.8, 4.4 and 5. The PDOP values are 3.3, 3.8 and 23 respectively (Shown in Table 14). Table 15 and 16 show that GLONASS cannot provide ambiguity fixed solutions for any marker. GPS provides fixed solutions for 40% of the markers (2 out of 5), and the fixed solution percentage is only 2% for each marker. The horizontal and vertical positioning errors are 0.020m and 0.044m respectively. BDS provides fixed solutions for 40% of the markers (2 out of 5). The horizontal and vertical positioning errors are 0.012m and 0.099m, and the fixed solution percentage is 8%. The GPS+GLONASS, GPS+BDS and GPS+BDS+GLONASS provide average 5.0%, 4.8% and 1% ambiguity fixed solutions and the RMS horizontal and vertical positioning errors are 0.025m and 0.067m, 0.009m and 0.011m, 0.007m and 0.071m respectively.

6.3.5 Positioning results for the markers in Category 5

Table 17 the number of visible satellites and DOP values for the markers in Category 5.

	GPS	GLONASS	BDS
--	-----	---------	-----

	No	PDOP	No	PDOP	No	PDOP
39	4	-	3	-	3	-
40	2	-	1	-	3	-
43	2	-	2	-	3	-
50	3	-	2	-	3	-

The 4 markers in Category 5 are in deep dense urban environments, the number of visible GPS, GLONASS and BDS are 2.75, 2 and 3. There are no ambiguity fixed solutions for the markers in Category 5.

7. An inertial based pipeline positioning technology

The inertial navigation technology can be applied for pipeline positioning with known start and end positions, which are usually measured by GNSS. The Ductrunner pipeline mapping system consists of two parts: a measure probe and two centralizing wheel sets (Figure 15). The measure probe contains 18 sensors including the gyroscopes, accelerometers, magnetometers, and thermometers. The centralizing wheel sets are used to travel inside the pipes with different diameter, and the back wheel set contains two odometers (Ductrunner 2014). The Ductrunner technology is gyroscopic pipeline mapping system. It travels inside an underground pipeline to estimate the trajectory of the Ductrunner, namely the pipeline position by integrating the IMU and odometer data, based on the known entry and exit coordinates. The Ductrunner positioning accuracy depends on the accuracy of entry and exit positions which are usually measured by GNSS. The advantages of the Ductrunner technology include: firstly it measures to any depth of buried pipes and ducts. Secondly, it can be used for both metallic and non-metallic pipes. Thirdly, it is insensitive to electromagnetic interference. Fourthly, it is able to position the pipes across river or underneath buildings. Lastly, if the GPS coordinates of entry and exit points of the pipe are provides, the Ductrunner can estimate the pipeline position with GPS coordinates, which is convenient for records. However, it can only travel through pipes which are empty, obstacles inside pipes will affect the positioning accuracy, and the accuracy will decrease for long pipes.



Figure 15 The Ductrunner pipeline mapping system.

7.1 test design and data collection

To evaluate the performance of the Ductrunner technology, a pipeline test site (Figure 16) has been established on the roof of SEB at UNNC. The total length of the test line is approximately 30m, and it consists of 5 x 6m pipes with 4 joint sockets. The shape of the test pipeline is designed as w shape to simulate more difficult situation compared with straight pipes. For the primary test, the pipeline is surveyed by using a Leica TS11 high accuracy total station to obtain precise 3D coordinates of the pipeline and provide 3D coordinates of the two end points for Ductrunner data post process. And then Ductrunner is pulled through the test pipeline manually to collect data.



Figure 16 the test pipeline.

7.2 Results and analysis

The pipeline position calculated by the Ductrunner software is compared to the true shape of the pipeline measured by the Leica TS11 total station. According to the test results, the maximum errors in horizontal plane and height are 0.080m and 0.040, which are 0.27% and 0.13% of the total pipeline length, respectively (Shown in Figure 17). The error increases from two ends to the middle of pipeline because forward and backward methods are used to estimate pipeline position with two known points at both ends of the pipeline.

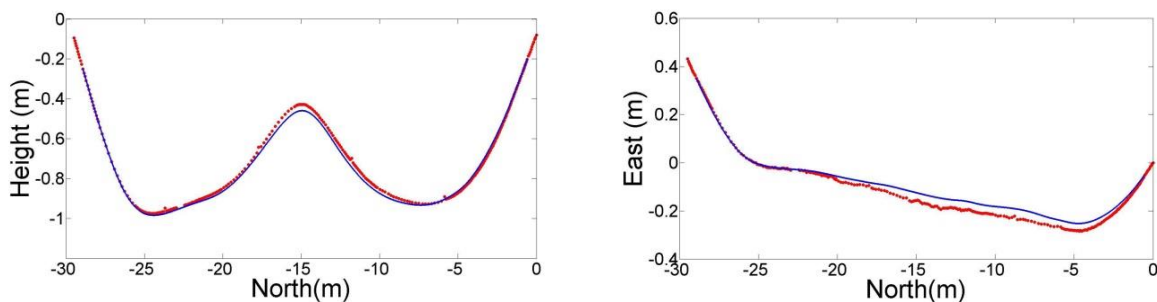


Figure 17 Comparison of pipeline positioning results between Ductrunner and total station in NH and NE planes (Red: Total station; Blue: Ductrunner).

The positioning results of the inertial technology for pipeline mapping depends on the accuracy of entry and exit coordinates, which are usually provided by GNSS to obtain absolute global positions. The GNSS static tests in urban environments show that 75% markers (21 out of 28) obtains ambiguity fixed solutions by different GNSS constellations. And the average horizontal and vertical positioning errors are less than 0.020m and 0.090m respectively. Adding the error of the inertial based pipeline positioning technology, the total error for pipeline positions is less than 0.150m, which is acceptable for underground utilities mapping. In addition, with the development of BDS and Galileo, and modernization of GLONASS, which will use CDMA instead of FDMA to increase the compatibility and interoperability with other GNSS constellation, it will improve the positioning availability and accuracy in urban areas. It will make contributions to efficiently obtain global positions of buried utilities with high accuracy.

8. Conclusions

After locating buried utilities, it is necessary to acquire and record the positions of them. GNSS including GPS, GLONASS, BDS, Galileo and QZSS are one of the most attractive positioning technologies to obtain absolute global positions. However, most of buried utilities are in urban area environments, where is not ideal for GNSS. In addition, inertial positioning technologies can be applied to estimate pipeline positions as well with known coordinates of start and end positions, which are usually provided by GNSS. To evaluate the availability, positioning precision and accuracy of different GNSS constellations, GNSS kinematic and static tests are carried out in a controlled environment. In addition, an approximately 30m long test pipeline has been established to evaluate the accuracy of an inertial based pipeline positioning technology.

In the GNSS kinematic test, the Leica GS10 positioning results show that GPS provides 24.7% ambiguity fixed solutions and GLONASS provides 18.5% ambiguity fixed solutions. The percentage of fixed solution is improved to 45.8% by integrating GPS and GLONASS. The positioning results of JAVAD Sigma receiver show that GPS and GLONASS provide a similar percentage of fixed solutions about 13%. Combining GPS and GLONASS, the number of fixed solution doubled. In addition, integrating GPS with only one QZSS satellite, which elevation angle is above 75 degrees during the test provides similar results compared with the GPS and GLONASS combination. The GNSS kinematic test results show that integrating multi-GNSS constellations improves the positioning results in urban area environments compared with a single GNSS constellation. In the GNSS static test, the markers in a controlled environment are divided into 5 categories from an open sky environment to dense urban environments. From open sky environment to dense urban environment, the number of visible GPS, GLONASS and BDS satellites decreases, the average number of visible GPS, GLONASS and BDS satellites decrease and the PDOP values increase. Moreover, the BDS PDOP value is larger than GPS and GLONASS PDOP values results from that the BDS constellation is not fully operational and has five geostationary satellites are always available but always in the same area of the sky. The bad BDS satellite geometry effects positioning accuracy for the 1st test on marker 21. In addition, the

number of ambiguity fixed solutions and positioning accuracy decrease from Category 1 to 5. GLONASS cannot provide ambiguity fixed solutions from Category 2 to 5. Although BDS constellation is not fully operational, and the geometry is not good, BDS provides similar positioning results compared with GPS with high elevation angles of five IGSO satellites during the test. Integration of GPS, GLONASS and BDS provides enough visible satellites in urban environments, but it does not always improve the positioning results. There are probably two reasons, one is that integration with GLONASS makes it difficult to obtain ambiguity fixed solutions, the other is that the combination of more satellites means higher chance to get multipath errors in urban environments.

There are 75% markers (21 out of 28) in the controlled urban environment provided with ambiguity fixed solutions either by GPS, BDS or GPS and BDS integration. Moreover, the maximum error is less than 10cm. For underground pipeline mapping, the positioning accuracy is acceptable. With the development of BDS, Galileo and other GNSS constellation, it is possible to obtain better result. In addition, it can provide reliable entry and exit coordinates, which is very important for the inertial based technology to obtain accurate pipeline positions.

REFERENCES

Gao, G.X. and Enge, P. (2012) How many GNSS satellites are too many? IEEE Trans. Aerosp. Electron. Syst. 48 (4), 2865–2874.

Costello, S.B., Chapman, D.N., Rogers, C.D.F. and Metje, N. (2007) Underground asset location and condition assessment technologies. *Tunnelling and Underground Space Technology*, 22, 524-542.

Ductrunner (2014) Ductrunner Technology Technical Method Statement. <http://www.reduct.net/>

Grewal, M.S., Andrews, A.P. and Bartone, C. (2013) *Global Navigation Satellite Systems, Inertial Navigation, and Integration*, 3rd ed. Wiley, Somerset, NJ, USA.

Groves, P.D. (2008) Principle of GNSS, Inertial and Multisensor Integrated Navigation Systems. Boston, London Artech House.

Hancock, C., Roberts, G. and Taha, A. (2009) Satellite mapping in cities: how good can it get? Proceedings of ICE, 122-128.

Hao, T., Rogers, C.D.F., Metje, N., Chapman, D.N., Muggleton, J.M., Foo, K.Y., Wang, P., Pennock, S.R., Atkins, P.R., Swingler, S.G., Parker, J., Costello, S.B., Burrow, M.P.N., Anspach, J.H., Armitage, R.J., Cohn, A.G., Goddard, K.F., Lewin, P.L., Orlando, G., Redfern, M.A., Royal, A.C.D. and Saul, A.J. (2012) Condition assessment of the buried utility service infrastructure. *Tunnelling and Underground Space Technology*, 28 (1), 331-344.

Liu, H., Xu, L., Shu, B., Zhang, M. and Qian, C. (2016) A new method to improve the performance of multi-GNSS pseudorange positioning in signal-degraded environment. Advances in Space Research 58, 577-586.

Hofmann-Wellenhof, B., Lichtenegger, H. and Wasle, E. (2008) GNSS—Global Navigation Satellite Systems: GPS, GLONASS, Galileo & more. Springer Wien New York.

Lau, L., Tateshita, H., and Sato, K. (2015). Impact of Multi-GNSS (GPS, GLONASS, and QZSS) on Positioning Accuracy and Multipath Errors in High-Precision Single-Epoch Solutions – A Case Study in Ningbo China. *The Journal of Navigation*, 68 (5), 999-1017.

Lester, J. and Bernold, L.E. (2007) Innovative process to characterize buried utilities using Ground Penetrating Radar. Automation in Construction, 16, 546-555.

Li, B., Feng, Y., Shen, Y. (2010) Three carrier ambiguity resolution: Distance-independent performance demonstrated using semi-generated triple frequency GPS signals. GPS Solutions. 14 (2), 177–184.

Liu, Y., Ge, M., Shi, C., Lou, Y., Wickert, J. and Schuh, H. (2016) Improving integer ambiguity resolution for GLONASS precise orbit determination. Journal of Geodesy, 90(8), 715-726.

McMahon, W., Burtwell, M.H. and Evans, M. (2006) *The Real Costs of Street Works to the Utility Industry and Society*. UK Water Industry Research Report No. 05/WM/12/8.

Metje, N., Atkins, P.R., Brennan, M.J., Chapman, D.N., Lim, H.M., Machell, J., Muggleton, J.M., Pennock, S., Ratcliffe, J., Redfern, M., Rogers, C.D.F., Saul, A.J., Shan, Q., Swingler, S. and Thomas, A.M. (2007) Mapping the Underworld—State-of-the-art review. *Tunnelling and Underground Space Technology*, 22, 568-586.

[Odijk, D. and Teunissen, P.J.G. \(2013\) Characterization of between-receiver GPS-Galileo inter-system biases and their effect on mixed ambiguity resolution. *GPS Solutions*, 17\(4\), 521–533.](#)

[O’Keefe, K., Petovello, M., Cao, W., Lachapelle, G. and Guyader, E. \(2009\) Comparing Multicarrier Ambiguity Resolution Methods for Geometry-Based GPS and Galileo Relative Positioning and Their Application to Low Earth Orbiting Satellite Attitude Determination, *International Journal of Navigation and Observation*, Article ID 592073, 15 pages, doi:10.1155/2009/592073](#)

Rizos, C., Higgins, M. and Hewitson, S. (2005) New GNSS Development and their Impact on Survey Service Provider and Surveyors. Proceedings of SSC2005 Spatial Intelligence, Innovation and Praxis: The national biennial Conference of the Spatial Sciences Institute. Melbourne, Spatial Sciences Institute, 1100-1113.

Roberts, G.W., Hancock, C., Ogundipe, O., Meng, X., Taha, A., Montillet, J.P. (2007) Positioning Buried Utilities using an integrated GNSS approach. Proceedings of International Global Navigation Satellite Systems Society Inc. The University of New South Wales, Sydney, Australia, 4-6 December.

[Royal, A.C.D., Atkins, P.R., Brennan, M.J., Chapman, D.N., Chen, H., Cohn, A.G., Foo, K.Y., Goddard, K.F., Hayes, R., Hao, T., Lewin, P.L., Metje, N., Muggleton, J.M., Naji, A., Orlando, G., Pennock, S.R., Redfern, M.A., Saul, A.J., Swingler, S.G., Wang, P. and Rogers, C.D.F. \(2011\) Site Assessment of Multiple-Sensor Approaches for Buried Utility Detection. *International Journal of Geophysics*, 1-19.](#)

[Savage, P.G. \(1998\) Strapdown Inertial Navigation Integration Algorithm Design Part 1: Attitude Algorithms. *Journal of Guidance, Control, and Dynamics*, 21\(1\), 19–28.](#)

[Taha, A., Hancock, C., Roberts, G.W. and Meng, X. \(2008\) The use of GPS and INS for centimetre precision during large GPS outages. Proceedings of International Symposium on GPS/GNSS, At Odaiba, Tokyo, Japan.](#)

[Takahashi, H. \(2004\) Japanese Regional Navigation Satellite System “The JRANS Concept”. *Journal of Global Positioning Systems*, 3\(1-2\), 259-264.](#)

Takasu. T. (2014) RTKLIB ver. 2.4.2 manual. <http://www.rtklib.com/prog/manual 2.4.2.pdf>

[Titterton, D.H. and Weston, J.L. \(1997\) Strapdown Inertial Navigation Technology. Lavenham, UK: The Lavenham Press Ltd.](#)

[Truong, D.M. and Tung, H.T. \(2013\) Development of real multi-GNSS positioning solutions and performance analyses. Proceedings of 2013 International Conference on Advanced Technologies for Communications \(ATC 2013\), Ho Chi Minh City, Vietnam, 158–163.](#)

[Zhang, P., Hancock, C., Lau, L., Roberts, G.W. and Xu, C. \(2016\) Integration of Low Cost IMU and Odometer for Underground Pipeline Mapping. Proceedings of the China Satellite Navigation Conference 2016, 18-20 May, Changsha, China.](#)